



HAL
open science

Phonon-Induced Pairing in Quantum Dot Quantum Simulator

Utso Bhattacharya, Tobias Grass, Adrian Bachtold, Maciej Lewenstein, Fabio Pistoiesi

► **To cite this version:**

Utso Bhattacharya, Tobias Grass, Adrian Bachtold, Maciej Lewenstein, Fabio Pistoiesi. Phonon-Induced Pairing in Quantum Dot Quantum Simulator. *Nano Letters*, 2021, 21 (22), pp.9661 - 9667. 10.1021/acs.nanolett.1c03457 . hal-03464766

HAL Id: hal-03464766

<https://hal.science/hal-03464766v1>

Submitted on 8 Dec 2021

HAL is a multi-disciplinary open access archive for the deposit and dissemination of scientific research documents, whether they are published or not. The documents may come from teaching and research institutions in France or abroad, or from public or private research centers.

L'archive ouverte pluridisciplinaire **HAL**, est destinée au dépôt et à la diffusion de documents scientifiques de niveau recherche, publiés ou non, émanant des établissements d'enseignement et de recherche français ou étrangers, des laboratoires publics ou privés.

Phonon-induced pairing in quantum dot quantum simulator

Utso Bhattacharya,^{1,2} Tobias Grass,¹ Adrian Bachtold,¹ Maciej Lewenstein,^{1,3} and Fabio Pistolesi⁴

¹*ICFO-Institut de Ciències Fotoniques, The Barcelona Institute of Science and Technology, Castelldefels (Barcelona) 08860, Spain.*

²*Max-Planck-Institut für Quantenoptik, D-85748 Garching, Germany*

³*ICREA, Pg. Lluis Companys 23, 08010 Barcelona, Spain*

⁴*Univ. Bordeaux, CNRS, LOMA, UMR 5798, F-33400 Talence, France*

Abstract: Quantum simulations can provide new insights into the physics of strongly correlated electronic systems. A well studied system, but still open in many regards, is the Hubbard-Holstein Hamiltonian, where electronic repulsion is in competition with attraction generated by the electron-phonon coupling. In this context we study the behavior of four quantum dots in a suspended carbon nanotube and coupled to its flexural degrees of freedom. The system is described by a Hamiltonian of the Hubbard-Holstein class, where electrons on different sites interact with the same phonon. We find that the system presents a transition from the Mott insulating state to a polaronic state, with the appearance of pairing correlations and the breaking of the translational symmetry. These findings will motivate further theoretical and experimental efforts to employ nanoelectromechanical systems to simulate strongly correlated systems with electron-phonon interactions.

Keywords: Quantum simulation, nanotubes, charge order, electron-phonon coupling, superconductivity

As for today, quantum simulators are the unique systems that can address, deepen our understanding, and ultimately solve with *quantum advantage* challenging problems of contemporary science: from quantum many body dynamics, through static and transient high T_c superconductivity to design of new materials. As an important example one can think to the Hubbard model, a paradigm of strongly correlated systems, and that has been investigated through a number of experimental platforms. Such platforms include arrays of three and four dots in semiconductor heterostructures [1, 2], as well as various setups used in the ultracold-atom community [3–11].

An important outstanding goal for quantum simulators is to go beyond pure Hubbard models by addressing also interactions between the particles with vibrations of the lattice, that is, with phonons. The electron-phonon (e-p) interactions can generate effective attractive electron-electron (e-e) interactions, via the Cooper pairing channel in conventional superconductors [12] and therefore, directly compete with the repulsive e-e interactions present. Such electron-phonon class of models (EPCM) are crucial for understanding a plethora of strongly correlated phases like antiferromagnetism, charge density waves, superconductivity, high-temperature superconductivity and the pseudogap states in low-dimensional materials, [13–16]. The interplay between the e-p interaction and the Coulombic e-e repulsion is also of great importance for unconventional superconductors such as alkali-metal-doped fullerides [17], pnictides [18, 19], and aromatic superconductors [20].

Since phonons are essentially absent in optical lattices, the study of EPCMs is challenging for atomic quantum simulators. Noteworthy in this context are the recent proposals for dynamical lattices [21, 22] and lattice gauge theory models, in which additional dynamical degrees of freedom on the bonds of the lattice (for reviews see

[23, 24]). On the other hand, electromechanical devices have been employed with great success to couple mechanical modes to quantum electron transport. In these systems the electrons can be localized in one (or two) quantum dots (QDs), and they interact electrostatically with one or several mechanical modes. The strong and controllable localization of the charge, with reduced screening, allows one to reach very large e-p coupling constant. This leads to strong back-action on the oscillator with the predicted formation of polaronic states and suppression of the conductance [25–28] and observed softening of the mechanical resonating frequency [29, 30]. Several transport regimes have been studied, such as single-electron tunneling [29–41], Kondo [42, 43] and the quantum Hall effect [44]. Several parameters of the Hamiltonian can be tuned independently, either at the fabrication stage or during the experiment. By tuning the nearby gate voltages, one can tune by a large amount the hopping term between the QDs, the local potential, and the e-p coupling. Advances in nanofabrication should soon enable the fabrication of several QDs (more than four) in a suspended carbon nanotube.

Therefore, electromechanical devices appear to be very promising as a new platform for simulating an EPCM. In this Letter, we scrutinize this novel quantum simulation platform, focusing on the concrete example of a phonon-induced delocalization transition. Given the theoretical interest in the EPCM, a tunable quantum simulator for such models is highly sought after, especially due to the restricted validity range of devised numerical and analytical approaches, such as quantum Monte Carlo [45], density-matrix renormalization group (DMRG) [46], variational ansatz [47, 48], dynamical mean-field theory (DMFT) [49], density-matrix embedding theory (DMET) [50].

In this Letter, we discuss in detail, within practical

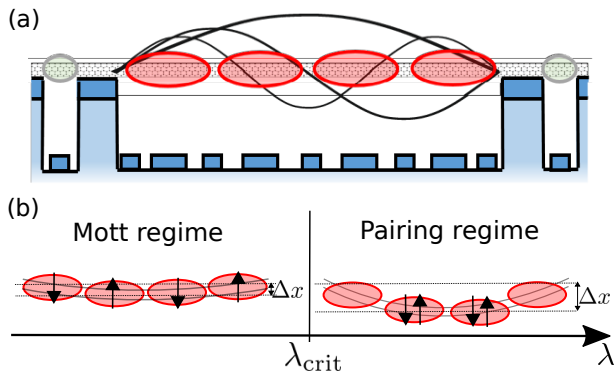


FIG. 1. (a) Schematic of the proposed setup: Four QDs in red are electrostatically defined along a suspended nanotube using the gate electrodes at the bottom of the trench. The electron states of the four QDs are coupled to the nanotube mechanical eigenmodes depicted as black lines. Real-time charge sensing of the QD array can be experimentally monitored with the sensing dots in grey defined on the sides [1]. (b) Illustration of the different regimes: Weak electron-phonon coupling ($\lambda < \lambda_{\text{crit}}$) supports a Mott state with one electron per dot; the small distortion Δx of the nanotube arises from the capacitive force when applying the voltage on the gate electrodes to form the quantum dots. In the presence of strong electron-phonon coupling ($\lambda > \lambda_{\text{crit}}$), the nanotube gets deformed by a larger amount and the electrons get paired in the two central dots.

experimental limits, the blueprint of a quantum simulation of an EPCM with e-e and e-p interactions using an electromechanical device. Specifically, we study the behavior of a system consisting of four QDs coupled to a set of phonons as a function of the e-p coupling constant and the hopping integral. In contrast to the well-studied Hubbard-Holstein model [51] with local e-p interaction, this setup realizes long range e-p interactions, as captured by the Hubbard-Froehlich model [52]. For vanishing hopping, the problem can be exactly solved, and a discontinuous transition from a Mott localized state to a symmetry breaking polaronic state with double occupancy of the central dots is observed. The sharp transition allows for a continuous evolution when the hopping terms are finite, with setting in of pairing and phonon correlations. The transition can be detected in the zero hopping limit by measuring the occupation of the different dots with nearby single-electron transistors [1] (Fig. 1). The obtained results indicate that the system is particularly rich and is interesting to investigate both experimentally and theoretically because of the correlated states generated by the interplay of the electronic and phononic degrees of freedom. Note that even in the experimentally most accessible and controllable regime of very low hopping, which is the focus of this Letter, there are phonon-induced fluctuations responsible for the interesting transition from Mott to polaronic states.

We consider a suspended carbon nanotube with four

equally spaced QDs (see Fig. 1). The quantum dots are electrostatically defined along the nanotube with voltages applied to the gate electrodes patterned at the bottom of the trench (Fig. 1), which enables the realization of well-defined quantum dots [53]. We assume a perfectly symmetric device, where the three hopping terms t between the four dots and local chemical potentials are equal. In this configuration the local Coulomb repulsion U is considered to be the same in each dot. We assume that the interdot Coulomb coupling is negligible. The system is prepared with only four electrons populating the dots. The tunnelling amplitude to the leads of the first and fourth dots is assumed to be negligible, so that the total number of electrons remain fixed. The charge on the dots naturally couples to the flexural modes of the carbon nanotube (see for instance [54]). The Hamiltonian describing the system belongs to the EPCM and therefore has a form: $H = H_e + H_p + H_{e-p}$. The electronic part is $H_e = H_t + H_U$ with $H_t = -t \sum_{i,\sigma} c_{i+1,\sigma}^\dagger c_{i,\sigma} + \text{h.c.}$ and a Hubbard term $H_U = \frac{U}{2} \sum_i n_i(n_i - 1)$, where $n_i = \sum_\sigma c_{i,\sigma}^\dagger c_{i,\sigma}$. Here, the index i represents the QDs, $\sigma = \pm$ accounts for the electrons' internal degree of freedom, and $c_{i,\sigma}$ are the destruction operators for the electronic states. We will focus on the case of two degrees of freedom, corresponding either to the valley degrees of freedom for the spin-polarized electrons, or the spin degrees of freedom when the valley symmetry is broken. The parameters t and U set the energy scale of hopping and on-site interaction. Since the system is isolated from the leads we can set the chemical potential to zero. The phonon part reads $H_p = \sum_\mu \hbar \omega_\mu a_\mu^\dagger a_\mu$. Here a_μ is the destruction operator for the flexural mode μ . We assume the limit of strong tension (guitar string limit) for which the resonating angular frequency $\omega_\mu = \mu \omega_0$ of the different modes is an integer multiple of the fundamental mode frequency ω_0 . The e-p coupling reads $H_{e-p} = \sum_{i,\mu} g_{i,\mu} n_i (a_\mu + a_\mu^\dagger)$, with its strength set by an electrostatically tunable parameter g_0 [28], and explicitly given by $g_{i,\mu} = g_0 \frac{8}{\pi} \mu^{-3/2} \sin[\pi\mu(2i-1)/8] \sin[\pi\mu/8]$. This expression is obtained by expanding the functional dependence of the capacitance, between each dot and the gate, on the displacement of the nanotube, and integrating it for the total dot extension, which is assumed to be 1/4 of the total nanotube length. The hopping term $t/(2\pi\hbar)$ and the electron phonon coupling $g/(2\pi\hbar)$ can be electrostatically tuned between 1 and 100 GHz and between 0.01 and 1 GHz, respectively. Here \hbar is the reduced Planck constant. The other parameters can be controlled by fabrication. Typically, the repulsion is $U/(2\pi\hbar) \sim 2$ THz, while the fundamental mode $\omega_0/(2\pi)$ can range between 1 MHz and 1 GHz. The hopping parameter t of each tunnel barrier and the chemical potential of each dot can independently be tuned by appropriately varying the applied voltage on the nine gate electrodes shown in Fig. 1, see also Ref. [55, 56]. The gate voltage, and

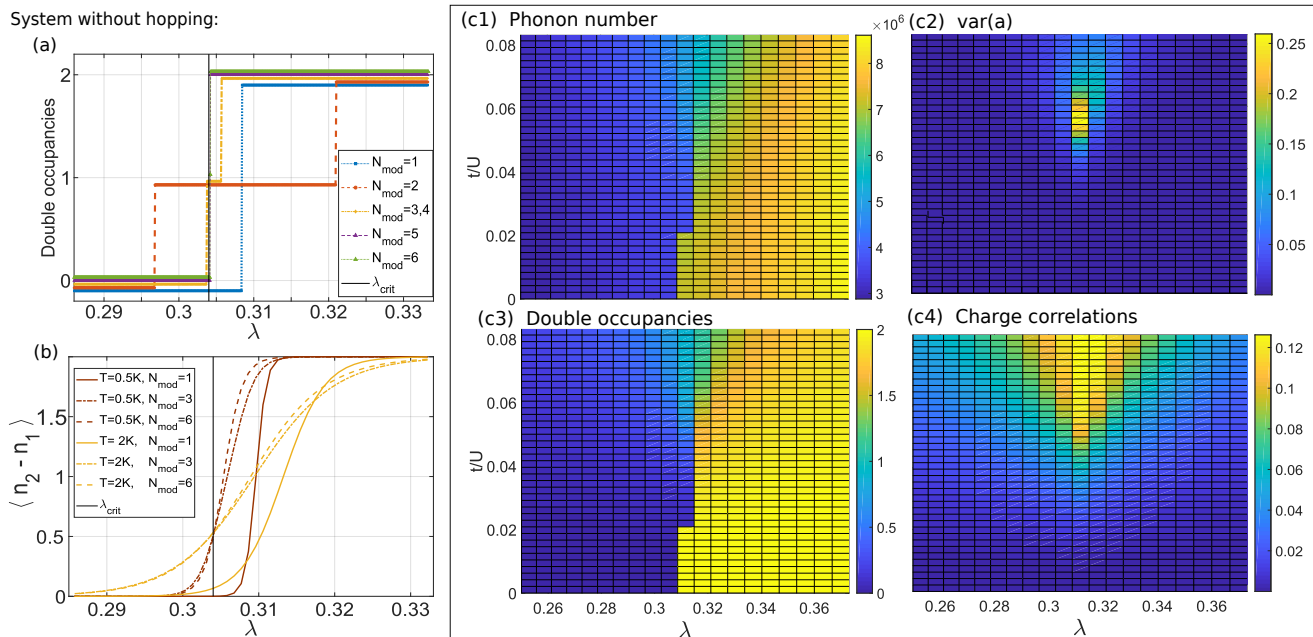


FIG. 2. (a,b) System behavior at $t = 0$: As a function of the dimensionless coupling parameter $\lambda = g_0^2/\omega U$, we plot the number of doubly occupied sites in the ground state (a), and the density contrast between dot 1 and dot 2, $\langle n_2 - n_1 \rangle$, at finite temperature (b). The extent of the intermediate regime (1 double occupancy), between the Mott state (no double occupancy) and the paired state (2 double occupancies), depends on the number of modes N_{mod} taken into consideration. The density contrast between these opposite regimes is clearly visible even at $T = 2K$. (c) System behavior at finite hopping: As a function λ and t , we plot (c1) the number of phonons, (c2) the variance of the phonon operator, (c3) the number of double occupancies, (c4) the average value of charge correlations in the ground state. We consider a system of four electrons in four dots, with $U/(2\pi\hbar) = 2400\text{GHz}$, and $\omega/(2\pi) = 1.35\text{MHz}$. In (c), we have restricted ourselves to a single-mode model, evaluated by exact diagonalization through iterated shift method in a Hilbert space of up to 30 phonons. Qualitatively, the parameter space at small t/U is divided into two localized regimes (Mott and paired regime), while at sufficiently large t/U a delocalized regime occurs, as indicated by finite charge correlations.

thus the electromechanical coupling, can also be tuned in a large range by changing the number N_s of filled shells, that is, by tuning the chemical potential such that the electron number changes from N to $N + 2N_d N_s$, where N_d is the number of QDs and the factor 2 accounts for the spin degeneracy.

Formally, the e-p coupling can be removed from the Hamiltonian by a Lang-Firsov (LF) transformation, $U = e^S$ with $S = \sum_{i,\mu} \frac{g_{i,\mu}}{\omega_\mu} n_i (a_\mu^\dagger - a_\mu)$. By applying this transformation accounts, the phonon coupling is accounted for through an additional effective interaction between electrons:

$$H_{\bar{U}} = - \sum_{\mu} \sum_{i,j} \frac{g_{i,\mu} g_{j,\mu}}{\omega_\mu} n_i n_j, \quad (1)$$

which is long-range due to the non-local nature of the phonons, and which can induce electron attraction. In addition to generating this effective potential, the LF transformation also modifies the effective hopping, making it prone to numerical instabilities. Therefore, we use the LF transformation only in the atomic limit, $t = 0$, where arbitrary numerical accuracy is possible.

In the atomic limit, the ground state is described by an

electronic Fock state, which is selected by the potential $H_U + H_{\bar{U}}$, times an *effective* phononic vacuum.

From the physical point of view the LF transformation allows to write the total energy of the system in terms of the displacement measured from the equilibrium position that minimizes the energy for given values of n_i . This generates the effective attractive polaronic potential since Eq. (1) is negative and quadratic in the number of particles. As illustrated in Fig. 1(b), two main regimes can be distinguished: (i) In the regime of weak electron-phonon coupling, the Hubbard repulsion H_U dominates over $H_{\bar{U}}$, and therefore the Mott-insulating configuration with one electron per dot is selected. (ii) In the regime of strong electron-phonon coupling, $H_{\bar{U}}$ is dominant, and the leading contribution from the $\mu = 1$ mode depletes the system on the outer dots and induces electron pairing on the inner dots. The system gains energy by the significant displacement of the nanotube.

For concreteness, let us consider in detail a nanotube with $N = 4$ QDs, at half-filling and unpolarized with respect to σ , i.e. we have $N/2$ electrons with $\sigma = +$, and $N/2$ electrons with $\sigma = -$. We introduce the dimensionless parameter $\lambda = g_0^2/(\omega U)$ which in the atomic limit

conveniently serves as a single control parameter of the system. We find that the $N!/[(N/2)!]^2 = 6$ Mott states (i.e. all states with occupation numbers $\{1, 1, 1, 1\}$) have energy $E/U = -\frac{2\pi^2}{3}\lambda$, and the unique paired state with occupation numbers $\{0, 2, 2, 0\}$ has $E/U = 2 - \frac{4\pi^2}{3}\lambda$. Accordingly, these two sets of states provide the electronic ground states of the system for any value of λ , with a level crossing at $\lambda_{\text{crit}} = 3/\pi^2$. We note that in this critical point, there are four additional ground states, referred to as “intermediate” states and characterized through occupation numbers $\{1, 2, 1, 0\}$ or $\{0, 1, 2, 1\}$ with an energy-dependence $E/U = 1 - \pi^2\lambda$. To obtain these expressions for the energies, we have carried out an infinite sum over the phonon modes, although for practical purposes one might instead truncate this sum at a finite number of modes N_{mod} . In this case, the scenario in the critical region is slightly altered: The degeneracy of three different types of density patterns (Mott, paired, intermediate) is lost. Instead, the intermediate states may appear above the ground states for any λ . This happens, e.g., for $N_{\text{mod}} = 1$ or $N_{\text{mod}} = 5$. Preferentially, though, the truncation of the modes gives rise to a tiny but finite parameter regime, in which the intermediate states become the unique ground states. This behavior is illustrated in Fig. 2(a), where the three regimes are distinguished by the number of doubly occupied sites in the ground state, plotted versus the dimensionless coupling parameter λ .

In practice, the number of doubly occupied dots is hard to quantify, since it would require simultaneous measurements of all local densities. However, as shown in Fig. 2(b), the density estimation on only two sites is sufficient to clearly distinguish between the different regimes. Concretely, we evaluate the density difference between an inner and an outer dot $\langle n_2 - n_1 \rangle$. This quantity takes the value 2 in the paired state, 1 in the intermediate state, and 0 in the Mott state. Here, instead of ground state averages, we have considered thermal averages at temperatures between 0.5K and 2K, assuming that the system’s energy scale is given by an interaction parameter $U/(2\pi\hbar) = 2400\text{GHz}$. Moreover, we have varied the number of modes, $N_{\text{mod}} = 1, 3, \text{ or } 6$. Importantly, in all cases and for all temperatures, the transition from Mott to paired state is clearly seen from this data, with a steeper change at $T = 0.5\text{K}$. At larger T , the intermediate regime broadens, and notably, the broadening is more pronounced in the 3- or 6-mode model than in the one-mode model, where the intermediate state is absent from the ground state manifold. In none of these cases, though, the intermediate state would give rise to a flat regime at $\langle n_2 - n_1 \rangle = 1$, demonstrating the secondary role played by the intermediate states.

The LF transformation can be viewed as a polaron dressing of the electrons, in which a certain electron occupation n_i implies the presence of $N_\mu = \langle a_\mu^\dagger a_\mu \rangle = \left(\sum_i n_i \frac{g_{i,\mu}}{\omega_\mu} \right)^2$ phonons in mode μ . From this number,

readily obtained at $t = 0$, we find valuable information also for the system at small but finite t . As mentioned above, numerical instability then prohibit the use of the LF transformation, and truncation of the phononic Hilbert space becomes necessary. According to the expression for N_μ , we find that, near criticality, the first (and most occupied) mode has $N_1 \approx (8\lambda_{\text{crit}}U/g_0)^2$ phonons. Thus, for the experimentally most relevant case of $U \gg g_0$, it is impossible to treat a Hilbert space with $\mathcal{O}(N_1)$ phonons.

Instead, we have developed an iterative shift method based on making the replacement

$$a_\mu \rightarrow \tilde{a}_\mu + S_\mu, \quad (2)$$

where \tilde{a}_μ is a shifted phonon operator, and S_μ is a complex number. If we choose $S_\mu = \sqrt{N_\mu}$, and numerically diagonalize the full Hamiltonian within a highly truncated Hilbert space of tilded phonons (e.g., $n_{\text{max}} \approx 30$), we recover, at $t = 0$, the same result as obtained before using the LF transformation. At finite t , the shift parameter S_μ has to be adjusted properly, which can be done iteratively: Using the $t = 0$ shift as an initial guess, we determine a new shift parameter

$$S'_\mu = \sqrt{\langle (\tilde{a}_\mu^\dagger + S_\mu^*)(\tilde{a}_\mu + S_\mu) \rangle_0}, \quad (3)$$

and repeat updating this parameter, until S_μ and S'_μ agree with the desired numerical precision. We have verified this method at small values of $U/g_0 \sim 1$, where a numerical procedure without shift is also possible, due to the relatively small number of phonons.

In the following, we report on our results for the experimentally realistic values $U/(2\pi\hbar) = 2400\text{GHz}$, being much larger than the phonon coupling strength g_0 (tunable, on the order of 1GHz [41]), and the phonon frequency, set to $\omega/(2\pi) = 1.35\text{MHz}$ in order to exploit the system near criticality. Such low resonance frequencies can be achieved in long nanotubes [57]. In this scenario, the phonon number is $\mathcal{O}(10^6)$, and therefore, we fully rely on the shift method.

Our results are shown in Fig. 2(c1–c4) for a one-mode model. The inclusion of more modes, is numerically challenging and expensive but does not alter the overall picture. Qualitatively, we find three regimes: At small t/U , there are the two localized regimes (Mott and paired regime), clearly distinguished by the occupation of the dots [e.g. number of double occupancies plotted in Fig. 2(c3)], but also through an abrupt change of the number of phonons [Fig. 2(c1)]. At sufficiently large t/U , a delocalized regime occurs, characterized through an intermediate phonon number and an intermediate number of doubly occupied dots. Interesting features of this third regime are finite values of electronic correlations, and the correlated phonon state. The latter is indicated by non-vanishing values of $\text{var}(a) \equiv \langle a^\dagger a \rangle - \langle a^\dagger \rangle \langle a \rangle$ [Fig. 2(c2)].

As an illustration of the electronic correlations, we plot in Fig. 2(c4) the average charge correlations C given by

$$C = \frac{1}{N} \sum_{i,j} (\langle n_i n_j \rangle_0 - \langle n_i \rangle_0 \langle n_j \rangle_0). \quad (4)$$

We note that in this regime, we have also obtained finite values of other pair correlators, such as s-wave or p-wave pairing correlators, $\langle S_i S_j \rangle_0$ or $\langle P_i P_j \rangle_0$, with $S_i^\dagger = c_{i\uparrow}^\dagger c_{i\downarrow}^\dagger$, and $P_i^\dagger = (c_{i+1\uparrow}^\dagger c_{i\downarrow}^\dagger + c_{i+1\downarrow}^\dagger c_{i\uparrow}^\dagger) / \sqrt{2}$.

The correlated nature makes the delocalized state at large t crucially different from the intermediate state at $t = 0$ discussed earlier, despite their similar structure of the density. We stress that the delocalized regime is *not* adiabatically connected to the intermediate $t = 0$ states, as we have checked (at a small value of U) by a three-mode calculation, which explicitly exhibits $t = 0$ intermediate states [cf. Fig. 1(a)]. Specifically, this calculation has shown that (i) finite values of t suppress the intermediate state until it fully vanishes, and that (ii) the delocalized regime, characterized by finite pair correlations, occurs only at even larger values of t . Intuitively, the suppression of the intermediate state by the hopping is understood from the extremely limited amount of first-order hopping which are possible in this configuration.

Any physical realization of the device implies a degree of static disorder induced by the unavoidable fabrication imperfections. One can expect that the "phase" diagram presented in Fig. 2 should be affected only for values of λ for which the difference in energy between the competing states is smaller than the typical energy scale \mathcal{E} of the static disorder. Using the estimate for vanishing t one finds that this region has a size $\delta\lambda \sim (3/\pi^2)\mathcal{E}/U$. When $\mathcal{E} \ll U$ this region is very small, indicating that the main picture is robust against weak disorder.

In summary, we have proposed an experimentally feasible way for quantum simulation of a Hamiltonian belonging to the EPCM, by placing four equally placed QDs in a suspended nanotube. A Mott state dominated by the e-e interaction, a polaronic state dominated by the e-p interaction, and a strongly correlated delocalized state at large hopping is observed. At small hopping, an intermediate state but not adiabatically connected to the strongly delocalized state is also found. The system has been theoretically explored by employing the Lang-Firsov transformation, which gives us analytically exact results for zero hopping, and by developing a numerically self-consistent iterative shift method. The distinction between the different regimes is done by looking at quantities such as the local electron density and e-e correlators, or the phonon distribution. These quantities in the finite hopping limit may be accessible in experiments where two of the dots are locally coupled to two different superconducting resonators [58]. Moreover, in the proposed experimental setup, the parameters are sufficiently tunable to explore the different regimes, and we find that

the stability of the states against finite temperatures is well within feasible temperature bounds.

Although this work focuses on the quantum simulation of the competition between the e-e and e-p coupling in four QDs embedded in a nanotube, it should be noted that our overall scheme is quite general. The first important extension would be to consider more dots. We focused on four because of current experimental capabilities. Albeit its reduced size, the system is already very rich. Ongoing advances in nanofabrication are expected to enable the fabrication of several QDs in suspended carbon nanotube, allowing to further investigate the evolution from the microscopic to the macroscopic system. Investigation of many intriguing scenarios are possible by controlling quantities like the number of electrons or dots, spin/valley degree of freedom, and the nature of mechanical modes (guitar string or doubly clamped beam without tensile tension). When filling $N/2$ electrons in N dots, the Peierls transition and charge density wave states may emerge with the help of the inter-dot Coulomb repulsion to prevent electrons to localize in nearby dots. Finally, by considering a current flowing through the nanotube, non-equilibrium physics could also be explored in the presence of e-p coupling, in such setups.

ACKNOWLEDGEMENTS

ICFO acknowledges support by Severo Ochoa (grant number SEV-2015-0522), Fundació Cellex, Fundació Mir-Puig, the CERCA Programme, the Fondo Europeo de Desarrollo Regional, European Social Fund. A.B. acknowledges support by ERC advanced (grant number 692876), ERC PoC (grant number 862149), AGAUR (grant number 2017SGR1664), MICINN (grant number RTI2018-097953-B-I00). M.L., U.B., and T.G. acknowledge support by ERC AdG NOQIA, Spanish Ministry MINECO and State Research Agency AEI (FIDEUA PID2019-106901GB-I00/10.13039 / 501100011033, and CEX2019-000910-S, FPI), Generalitat de Catalunya (AGAUR Grant No. 2017 SGR 1341, Quantum-CAT U16-011424, co-funded by ERDF Operational Program of Catalonia 2014-2020), MINECO-EU QUANTERA MAQS (funded by State Research Agency (AEI) PCI2019-111828-2 / 10.13039/501100011033), EU Horizon 2020 FET-OPEN OPTOLogic (Grant No 899794), and the National Science Centre, Poland-Symfonia Grant No. 2016/20/W/ST4/00314. T.G. acknowledges funding from "la Caixa" Foundation (ID 100010434, fellowship code LCF/BQ/PI19/11690013). U.B. acknowledges support by the "Cellex-ICFO-MPQ Research Fellows", a joint program between ICFO and MPQ – Max-Planck-Institute for Quantum Optics, funded by the Fundació Cellex. F.P. acknowledges support from the French Agence Nationale de la Recherche (grant SINPHOCOM ANR-19-CE47-0012) and IDEX Bordeaux (grant Maesim

Risky project 2019 of the LAPHIA Program).

REFERENCES

- [1] T. Hensgens, T. Fujita, L. Janssen, Xiao Li, C. J. Van Diepen, C. Reichl, W. Wegscheider, S. Das Sarma, and L. M. K. Vandersypen, “Quantum simulation of a fermi–hubbard model using a semiconductor quantum dot array,” *Nature* **548**, 70–73 (2017).
- [2] J. P. Dehollain, U. Mukhopadhyay, V. P. Michal, Y. Wang, B. Wunsch, C. Reichl, W. Wegscheider, M. S. Rudner, E. Demler, and L. M. K. Vandersypen, “Nagaoka ferromagnetism observed in a quantum dot plaquette,” *Nature* **579**, 528–533 (2020).
- [3] Anton Mazurenko, Christie S. Chiu, Geoffrey Ji, Maxwell F. Parsons, Márton Kanász-Nagy, Richard Schmidt, Fabian Grusdt, Eugene Demler, Daniel Greif, and Markus Greiner, “A cold-atom fermi–hubbard anti-ferromagnet,” *Nature* **545**, 462–466 (2017).
- [4] Christie S. Chiu, Geoffrey Ji, Anton Mazurenko, Daniel Greif, and Markus Greiner, “Quantum state engineering of a hubbard system with ultracold fermions,” *Phys. Rev. Lett.* **120**, 243201 (2018).
- [5] Christie S. Chiu, Geoffrey Ji, Annabelle Bohrdt, Muqing Xu, Michael Knap, Eugene Demler, Fabian Grusdt, Markus Greiner, and Daniel Greif, “String patterns in the doped hubbard model,” *Science* **365**, 251–256 (2019), <https://science.sciencemag.org/content/365/6450/251.full.pdf>
- [6] Annabelle Bohrdt, Christie S. Chiu, Geoffrey Ji, Muqing Xu, Daniel Greif, Markus Greiner, Eugene Demler, Fabian Grusdt, and Michael Knap, “Classifying snapshots of the doped hubbard model with machine learning,” *Nature Physics* **15**, 921–924 (2019).
- [7] Geoffrey Ji, Muqing Xu, Lev Haldar Kendrick, Christie S. Chiu, Justus C. Brüggengjürgen, Daniel Greif, Annabelle Bohrdt, Fabian Grusdt, Eugene Demler, Martin Lebrat, and Markus Greiner, “Coupling a mobile hole to an antiferromagnetic spin background: Transient dynamics of a magnetic polaron,” *Phys. Rev. X* **11**, 021022 (2021).
- [8] S. Trotzky, P. Cheinet, S. Fölling, M. Feld, U. Schnorrberger, A. M. Rey, A. Polkovnikov, E. A. Demler, M. D. Lukin, and I. Bloch, “Time-resolved observation and control of superexchange interactions with ultracold atoms in optical lattices,” *Science* **319**, 295 (2008).
- [9] Frederik Görg, Michael Messer, Kilian Sandholzer, Gregor Jotzu, Rémi Desbuquois, and Tilman Esslinger, “Enhancement and sign change of magnetic correlations in a driven quantum many-body system,” *Nature* **553**, 481–485 (2018).
- [10] Guillaume Salomon, Joannis Koepsell, Jayadev Vijayan, Timon A. Hilker, Jacopo Nespolo, Lode Pollet, Immanuel Bloch, and Christian Gross, “Direct observation of incommensurate magnetism in hubbard chains,” *Nature* **565**, 56–60 (2019).
- [11] Matthew A. Nichols, Lawrence W. Cheuk, Melih Okan, Thomas R. Hartke, Enrique Mendez, T. Senthil, Ehsan Khatami, Hao Zhang, and Martin W. Zwierlein, “Spin transport in a mott insulator of ultracold fermions,” *Science* **363**, 383 (2019).
- [12] J. Bardeen, L. N. Cooper, and J. R. Schrieffer, “Theory of superconductivity,” *Phys. Rev.* **108**, 1175–1204 (1957).
- [13] Seher Karakuzu, Luca F. Tocchio, Sandro Sorella, and Federico Becca, “Superconductivity, charge-density waves, antiferromagnetism, and phase separation in the Hubbard-Holstein model,” *Phys. Rev. B* **96**, 205145 (2017).
- [14] A Lanzara, PV Bogdanov, XJ Zhou, SA Kellar, DL Feng, ED Lu, T Yoshida, H Eisaki, Atsushi Fujimori, K Kishio, *et al.*, “Evidence for ubiquitous strong electron–phonon coupling in high-temperature superconductors,” *Nature* **412**, 510–514 (2001).
- [15] Sergi Julià-Farré, Alexandre Dauphin, Ravindra W. Chhajlany, Piotr T. Grochowski, Simon Wall, Maciej Lewenstein, and Przemysław R. Grzybowski, “Nanoscale phase separation and pseudogap in the hole-doped cuprates from fluctuating cu-o-cu bonds,” *Phys. Rev. B* **101**, 125107 (2020).
- [16] KM Shen, F Ronning, DH Lu, WS Lee, NJC Ingle, W Meevasana, F Baumberger, A Damascelli, NP Armitage, LL Miller, *et al.*, “Missing quasiparticles and the chemical potential puzzle in the doping evolution of the cuprate superconductors,” *Physical review letters* **93**, 267002 (2004).
- [17] Yasuhiro Takabayashi, Alexey Y. Ganin, Peter Jeglič, Denis Arčon, Takumi Takano, Yoshihiro Iwasa, Yasuo Ohishi, Masaki Takata, Nao Takeshita, Kosmas Prassides, and Matthew J. Rosseinsky, “The disorder-free non-bcs superconductor CsCuOCl emerges from an antiferromagnetic insulator parent state,” *Science* **323**, 1585 (2009).
- [18] Clarina de la Cruz, Q. Huang, J. W. Lynn, Jiyang Li, W. Ratcliff II, J. L. Zarestky, H. A. Mook, G. F. Chen, J. L. Luo, N. L. Wang, and Pengcheng Dai, “Magnetic order close to superconductivity in the iron-based layered $\text{LaO}_{1-x}\text{F}_x$ systems,” *Nature* **453**, 899–902 (2008).
- [19] Hiroshi Kontani and Seiichiro Onari, “Orbital-fluctuation-mediated superconductivity in iron pnictides: Analysis of the five-orbital hubbard-holstein model,” *Phys. Rev. Lett.* **104**, 157001 (2010).
- [20] Ryoji Mitsuhashi, Yuta Suzuki, Yusuke Yamanari, Hiroki Mitamura, Takashi Kambe, Naoshi Ikeda, Hideki Okamoto, Akihiko Fujiwara, Minoru Yamaji, Naoko Kawasaki, Yutaka Maniwa, and Yoshihiro Kubozono, “Superconductivity in alkali-metal-doped picene,” *Nature* **464**, 76–79 (2010).
- [21] U. Bissbort, D. Cocks, A. Negretti, Z. Idziaszek, T. Calarco, F. Schmidt-Kaler, W. Hofstetter, and R. Gerritsma, “Emulating solid-state physics with a hybrid system of ultracold ions and atoms,” *Phys. Rev. Lett.* **111**, 080501 (2013).
- [22] Daniel González-Cuadra, Przemysław R. Grzybowski, Alexandre Dauphin, and Maciej Lewenstein, “Strongly correlated bosons on a dynamical lattice,” *Phys. Rev. Lett.* **121**, 090402 (2018).
- [23] Mari Carmen Bañuls, Rainer Blatt, Jacopo Catani, Alessio Celi, Juan Ignacio Cirac, Marcello Dalmonte, Leonardo Fallani, Karl Jansen, Maciej Lewenstein, Simone Montangero, Christine A. Muschik, Benni Reznik, Enrique Rico, Luca Tagliacozzo, Karel Van Acoleyen, Frank Verstraete, Uwe-Jens Wiese, Matthew Wingate, Jakub Zakrzewski, and Peter Zoller, “Simulating lattice gauge theories within quantum technologies,” *The European Physical Journal D* **74**, 165 (2020).
- [24] Monika Aidelsburger, Luca Barbiero, Alejandro Bermudez, Titas Chanda, Alexandre Dauphin, Daniel

- González-Cuadra, Przemysław R. Grzybowski, Simon Hands, Fred Jendrzejewski, Johannes Jünemann, Gediminas Juzeliunas, Valentin Kasper, Angelo Piga, Shi-Ju Ran, Matteo Rizzi, German Sierra, Luca Tagliacozzo, Emanuele Tirrito, Torsten V. Zache, Jakub Zakrzewski, Erez Zohar, and Maciej Lewenstein, “Cold atoms meet lattice gauge theory,” (2021), 2106.03063. Arxiv. arxiv.org/pdf/2106.03063.pdf (accessed 11/02/2021).
- [25] Michael Galperin, Mark A. Ratner, and Abraham Nitzan, “Hysteresis, Switching, and Negative Differential Resistance in Molecular Junctions: A Polaron Model,” *Nano Lett.* **5**, 125–130 (2005).
- [26] Jens Koch and Felix von Oppen, “Franck-Condon Blockade and Giant Fano Factors in Transport through Single Molecules,” *Phys. Rev. Lett.* **94**, 206804 (2005).
- [27] F. Pistolesi, Ya. M. Blanter, and Ivar Martin, “Self-consistent theory of molecular switching,” *Physical Review B* **78** (2008), 10.1103/PhysRevB.78.085127.
- [28] G. Micchi, R. Avriller, and F. Pistolesi, “Mechanical Signatures of the Current Blockade Instability in Suspended Carbon Nanotubes,” *Phys. Rev. Lett.* **115**, 206802 (2015).
- [29] B. Lassagne, Y. Tarakanov, J. Kinaret, D. Garcia-Sanchez, and A. Bachtold, “Coupling Mechanics to Charge Transport in Carbon Nanotube Mechanical Resonators,” *Science* **325**, 1107–1110 (2009).
- [30] G. A. Steele, A. K. Hüttel, B. Witkamp, M. Poot, H. B. Meerwaldt, L. P. Kouwenhoven, and H. S. J. van der Zant, “Strong Coupling Between Single-Electron Tunneling and Nanomechanical Motion,” *Science* **325**, 1103–1107 (2009).
- [31] Michael T. Woodside and Paul L. McEuen, “Scanned probe imaging of single-electron charge states in nanotube quantum dots,” *Science* **296**, 1098–1101 (2002), <https://science.sciencemag.org/content/296/5570/1098.full.pdf>.
- [32] Robert G. Knobel and Andrew N. Cleland, “Nanometre-scale displacement sensing using a single electron transistor,” *Nature* **424**, 291–293 (2003).
- [33] A. Naik, O. Buu, M. D. LaHaye, A. D. Armour, A. A. Clerk, M. P. Blencowe, and K. C. Schwab, “Cooling a nanomechanical resonator with quantum back-action,” *Nature* **443**, 193–196 (2006).
- [34] Marc Ganzhorn and Wolfgang Wernsdorfer, “Dynamics and dissipation induced by single-electron tunneling in carbon nanotube nanoelectromechanical systems,” *Phys. Rev. Lett.* **108**, 175502 (2012).
- [35] A. Benyamini, A. Hamo, S. Viola Kusminskiy, F. von Oppen, and S. Ilani, “Real-space tailoring of the electron-phonon coupling in ultraclean nanotube mechanical resonators,” *Nat. Phys.* **10**, 151–156 (2014).
- [36] J.-M. Pirkkalainen, S.U. Cho, F. Massel, J. Tuorila, T.T. Heikkilä, P.J. Hakonen, and M.A. Sillanpää, “Cavity optomechanics mediated by a quantum two-level system,” *Nature Communications* **6** (2015), 10.1038/ncomms7981.
- [37] N. Ares, T. Pei, A. Mavalankar, M. Mergenthaler, J. H. Warner, G. A. D. Briggs, and E. A. Laird, “Resonant Optomechanics with a Vibrating Carbon Nanotube and a Radio-Frequency Cavity,” *Physical Review Letters* **117** (2016), 10.1103/PhysRevLett.117.170801.
- [38] Ilya Khivrich, Aashish A. Clerk, and Shahal Ilani, “Nanomechanical pump-probe measurements of insulating electronic states in a carbon nanotube,” *Nat. Nanotechnol.* **14**, 161–167 (2019).
- [39] Yutian Wen, N. Ares, F. J. Schupp, T. Pei, G. a. D. Briggs, and E. A. Laird, “A coherent nanomechanical oscillator driven by single-electron tunnelling,” *Nat. Phys.* **16**, 75–82 (2020).
- [40] Stefan Blien, Patrick Steger, Niklas Hüttner, Richard Graaf, and Andreas K. Hüttel, “Quantum capacitance mediated carbon nanotube optomechanics,” *Nat. Comm.* **11**, 1636 (2020).
- [41] Florian Vigneau, Juliette Monsel, Jorge Tabanera, Léa Bresque, Federico Fedele, G. A. D. Briggs, Janet Anders, Juan M. R. Parrondo, Alexia Auffèves, and Natalia Ares, “Ultrastrong coupling between electron tunneling and mechanical motion,” (2021), 2103.15219. Arxiv. arxiv.org/pdf/2103.15219.pdf (accessed 11/02/2021).
- [42] K. J. G. Götz, D. R. Schmid, F. J. Schupp, P. L. Stiller, Ch. Strunk, and A. K. Hüttel, “Nanomechanical characterization of the kondo charge dynamics in a carbon nanotube,” *Phys. Rev. Lett.* **120**, 246802 (2018).
- [43] C. Urgell, W. Yang, S. L. De Bonis, C. Samanta, M. J. Esplandiú, Q. Dong, Y. Jin, and A. Bachtold, “Cooling and self-oscillation in a nanotube electromechanical resonator,” *Nat. Phys.* **16**, 32–37 (2020).
- [44] Changyao Chen, Vikram V. Deshpande, Mikito Koshino, Sunwoo Lee, Alexander Gondarenko, Allan H. MacDonald, Philip Kim, and James Hone, “Modulation of mechanical resonance by chemical potential oscillation in graphene,” *Nature Physics* **12**, 240–244 (2016).
- [45] RT Clay and RP Hardikar, “Intermediate phase of the one dimensional half-filled hubbard-holstein model,” *Physical review letters* **95**, 096401 (2005).
- [46] H Fehske, G Hager, and E Jeckelmann, “Metallicity in the half-filled holstein-hubbard model,” *EPL (Europhysics Letters)* **84**, 57001 (2008).
- [47] BJ Alder, KJ Runge, and RT Scalettar, “Variational monte carlo study of an interacting electron-phonon model,” *Physical review letters* **79**, 3022 (1997).
- [48] Yao Wang, Ilya Esterlis, Tao Shi, J. Ignacio Cirac, and Eugene Demler, “Zero-temperature phases of the two-dimensional hubbard-holstein model: A non-gaussian exact diagonalization study,” *Phys. Rev. Research* **2**, 043258 (2020).
- [49] Philipp Werner and Andrew J Millis, “Efficient dynamical mean field simulation of the holstein-hubbard model,” *Physical review letters* **99**, 146404 (2007).
- [50] Barbara Sandhoefer and Garnet Kin-Lic Chan, “Density matrix embedding theory for interacting electron-phonon systems,” *Physical Review B* **94**, 085115 (2016).
- [51] G. Beni, P. Pincus, and J. Kanamori, “Low-temperature properties of the one-dimensional polaron band. i. extreme-band-narrowing regime,” *Phys. Rev. B* **10**, 1896–1901 (1974).
- [52] A. S. Alexandrov and P. E. Kornilovitch, “The Fröhlich-Coulomb model of,” *J. Phys.: Condens. Matter* **14**, 5337–5348 (2002).
- [53] J. Waissman, M. Honig, S. Pecker, A. Benyamini, A. Hamo, and S. Ilani, “Realization of pristine and locally tunable one-dimensional electron systems in carbon nanotubes,” *Nature Nanotechnology* **8**, 569–574 (2013).
- [54] F. Pistolesi, A. N. Cleland, and A. Bachtold, “Proposal for a nanomechanical qubit,” *Phys. Rev. X* **11**, 031027 (2021).
- [55] R. Durrer, B. Kratochwil, J.V. Koski, A.J. Landig, C. Reichl, W. Wegscheider, T. Ihn, and E. Greplova, “Automated tuning of double quantum dots into specific charge states using neural networks,” *Phys. Rev. Applied* **13**,

- 054019 (2020).
- [56] T.-K. Hsiao, C.J. van Diepen, U. Mukhopadhyay, C. Reichl, W. Wegscheider, and L.M.K. Vandersypen, “Efficient orthogonal control of tunnel couplings in a quantum dot array,” *Phys. Rev. Applied* **13**, 054018 (2020).
- [57] J. Moser, J. Güttinger, A. Eichler, M. J. Esplandiu, D. E. Liu, M. I. Dykman, and A. Bachtold, “Ultra-sensitive Force Detection with a Nanotube Mechanical Resonator,” *Nat Nanotech* **8**, 493 (2013).
- [58] J. J. Viennot, M. C. Dartailh, A. Cottet, and T. Kontos, “Coherent coupling of a single spin to microwave cavity photons,” *Science* **349**, 408–411 (2015).